Defense Technical Information Center Compilation Part Notice

ADP012081

TITLE: Dynamic Processes of Supercavitation and Computer Simulation

DISTRIBUTION: Approved for public release, distribution unlimited

This paper is part of the following report:

TITLE: Supercavitating Flows [les Ecoulements supercavitants]

To order the complete compilation report, use: ADA400728

The following component part numbers comprise the compilation report:
ADP012072 thru ADP012091

Dynamic Processes of Supercavitation and Computer Simulation

Vladimir N. Semenenko
National Academy of Sciences – Institute of Hydromechanics
8/4 Zhelyabov str., Kyiv, 03057
Ukraine

Summary

This lecture is devoted to unsteady processes in the flows with natural and artificial supercavitation. We consider two classes of phenomena:

1) forced non-stationarity of the flow which is induced by external causes – a model velocity change, an ambient pressure impulse, a variation of gas supply into a cavity etc.;

2) self-exited oscillation arising due to internal instability of gas-filled supercavities.

Results of computer simulation of the dynamic supercavitation processes are presented. They were obtained by using the approximate mathematical model based on the G.Logvinovich independence principle of the supercavity expansion.

A comparison of unsteady behaviour of axisymmetric and two-dimensional supercavities is given. Formulation and solution of two 2-D problems are presented:

1) the problem on instability of the 2-D gas-filled supercavity;

2) the problem on evolution of the 2-D supercavity past an oscillating wedge.

The solutions are based on the M.Tulin's linearized cavitation scheme.

The lecture material is illustrated by sequences of motion-picture frames and photographs of the unsteady supercavitation processes. They were obtained at the hydrodynamic laboratory of the Institute of Hydromechanics of NAS of Ukraine (IHM UNAS).

1 Main types of dynamic supercavitation processes

We consider main types of the supercavitation flows and characteristic for each of them unsteady phenomena which are well simulated by using the accepted mathematical model.

1.1 SUPERCAVITY FORMATION DURING HIGH–SPEED WATER ENTRY

When the high-speed motion in water is experimentally investigated at the IHM UNAS, models are accelerated with the vapor-gas catapult up to velocities 500 ÷ 1400 m/sec, enter into water through the membrane and then move under water on inertia in the natural super-cavitation regime [1, 2]. Length of the distance is 35 m.

Fig. 1 shows consecutive frames of the initial period of the model motion. The cell of the coordinate mesh is 0.2 × 0.2 m. The cavitator diameter of model is D_n = 1.5 mm, the model velocity is V_0 = 980 m/sec. One can see that the cavity formation process has a stage of cavity closure caused by rapid increase of the water pressure when the model and gases penetrate into water. In this case, if a stability of the model motion does not loss, then the normal formation of the supercavity goes on in further.

Paper presented at the RTO AVT Lecture Series on "Supercavitating Flows", held at the von Kármán Institute (VKI) in Brussels, Belgium, 12-16 February 2001, and published in RTO EN-010.

1.2 NATURAL HIGH–SPEED SUPERCAVITIES

A main characteristic peculiarity of high-speed super-cavities is their very huge aspect ratio $\lambda = L_c / D_c = 70 \div 200$, where L_c is the cavity length; D_c is the cavity mid-section diameter. The vapor cavitation number is unique similarity parameter for such flows:

$$\sigma = \frac{2(p_\infty - p_v)}{\rho V^2}, \qquad (1)$$

where p_∞ is the pressure at infinity; $p_v = 2350$ Pascal is the saturated water vapor pressure (at the temperature 20 °C); ρ is the water density. This type of flow corresponds to the cavitation numbers $\sigma < 10^{-3}$.

Fig. 2 shows a sequence of frames of shooting the high-speed supercavity ($D_n = 1.2$ mm; $V = 1075$ m/sec; $L_c = 18$ m). The shooting frequency in this experiment was $N = 4200$ frames/sec, the time interval between the frames was $1 / N = 0.24$ msec.

A typical unsteady process at the high-speed motion of the supercavitating model on inertia is fast decrease of both the velocity and the cavity length. The super-cavitation regime of motion remains until the model is fully placed within the cavity.

The second peculiarity of the high-speed super-cavities is the cavity closure mechanism. The cavities in the described experiments fluently closed practically in a point in contrast to the vapor cavities when cavitation numbers $\sigma < 0.01$. For latter, the unsteady closure with periodic arising reentrant jet is characteristic. It is seen from sequential frames of the experiments that the wake past the cavities has periodic bubble structure. Absolute frequencies of the periodic structure in the wake were in range 80 ÷ 140 kHz in various experiments when $D_n = 1.2 \div 1.5$. In Fig. 2, the frequency is equal to 140 kHz .

The analysis showed that one of causes of the periodic bubble wake formation may be elastic vibrations of the model.

The third peculiarity of the high-speed supercavitation motion in water is the stability mechanism of motion. For the supercavitating models, the classical condition of the motion stability in continuum is not fulfilled. It consists in location of the point of the hydrodynamic force application past the center of the body mass. The experiments showed that the stabilization of free motion of the supercavitating models is attained owing to ricocheting the model tail from the inner cavity walls when $V > 300$ m/sec [1, 2].

In the experiment, action of this stabilization mechanism appears in periodic perturbations of the supercavity surface that develop according to the independence principle. In Fig. 3, two experimental photographs are showed: the model at the time of touching the upper internal cavity wall (a) and the cavity part perturbed owing to contact with the model (b). Exposure time for shooting was $3 \cdot 10^{-6}$ sec.

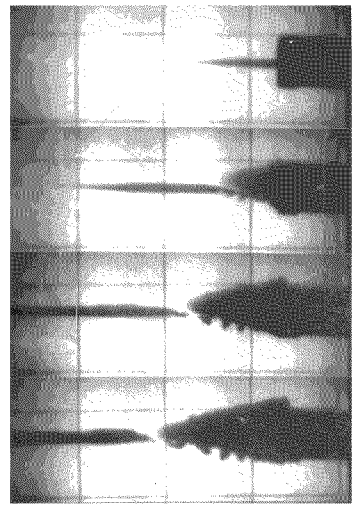

Fig. 1. High-speed water entry: D_n = 1.5 mm, V_0 = 980 m/sec

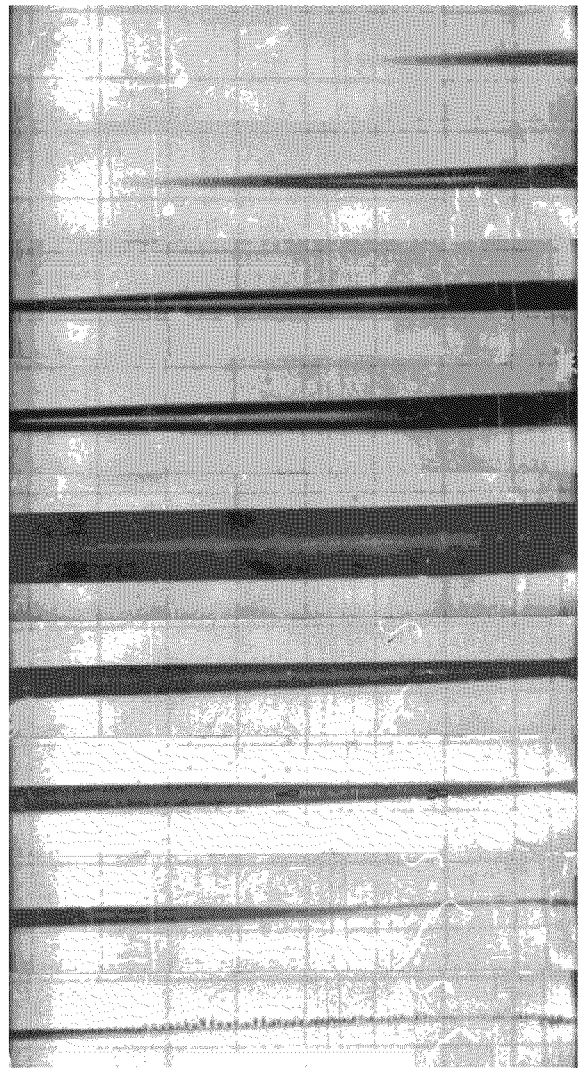

Fig. 2. High-speed supercavity: D_n = 1.2 mm; V = 1075 m/sec

1.3. ARTIFICIAL VENTILATED CAVITIES

The supercavitation regime may be created in water at the moderate velocities $V = 10 \div 100$ m/sec. The basic similarity parameters of the ventilation flow are:

$$\sigma = \frac{2(p_\infty - p_c)}{\rho V^2}, \quad Fr = \frac{V}{\sqrt{gD_n}}, \quad \beta = \frac{\sigma_v}{\sigma}, \tag{2}$$

where $p_c > p_v$ is the cavity pressure; Fr is the Froude number; g is the gravity acceleration; D_n is the cavitator diameter. The cavitation numbers $10^{-2} < \sigma < 0.1$ correspond to this type of flow.

The Froude number Fr characterizes the distorting effect of the gravity on the cavity shape. Estimations show that it is considerable when $\sigma Fr < 2$ [3].

The dynamic similarity parameter $\beta \geq 1$, that is equal to relation of the vapor cavitation number σ_v and its real value σ, plays an important role at calculation of the unsteady ventilation flow.

The value $\beta = 1$ corresponds to the natural supercavitation. When the parameter β increases, significance of elasticity of the gas filling the ventilated cavity increases as well.

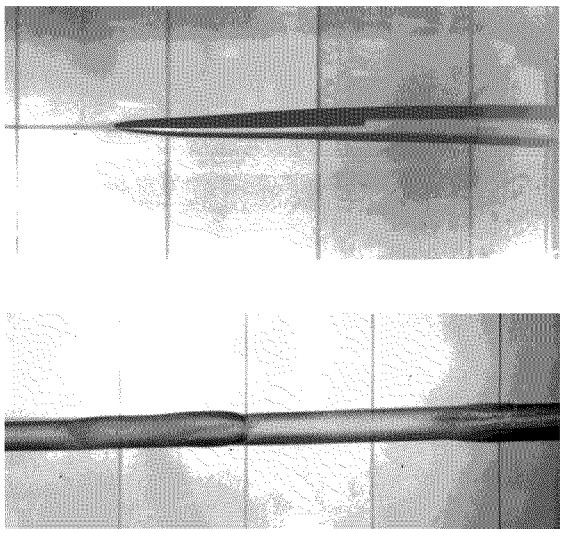

Fig. 3. Cavity perturbation at ricocheting: $D_n = 3$ mm, $V = 690$ m/ sec

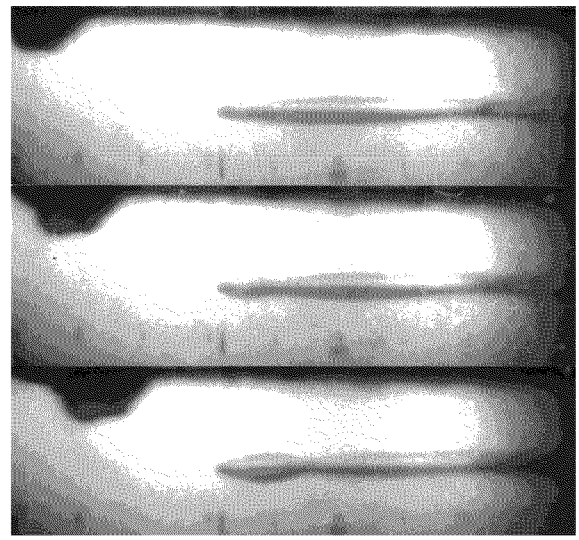

Fig. 4. Ventilated cavity reaction on the pressure impulse: $D_n = 20$ mm, $V = 9$ m/sec

Fig. 4 shows a sequence of motion-picture frames of the ventilated cavity deformation under action of the ambient pressure impulse. The pressure impulse in water was created with the compressed-air catapult. The air bubble created by the catapult is seen in the upper part of the frames. The frames show that the pressure impulse results in the axisymmetric pinch of the cavity.

A characteristic unsteady process for ventilated cavities is the cavity evolution at changing or ceasing the gas-supply. The experiments show that this process is determined by type of the gas-leakage from the cavity [3, 4]. In Fig.5, the typical experimental graphs of $L_c(t)$, $D_c(t)$ are shown when the air-supply was instantly turned on and turned off [5]. The portion type of the air-leakage from the cavity was maintained during this test. It is seen that the cavity length increased by linear law. This process was

decelerated only at approach to the stationary regime. On the contrary, the cavity decreased with increasing speed when the cavity closes.

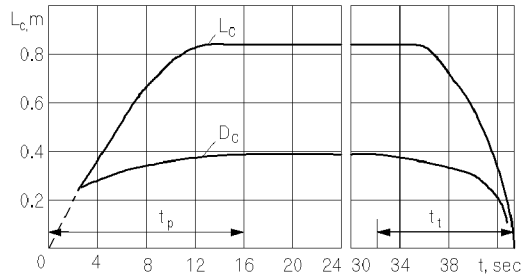

Fig. 5. Ventilated cavity history at air-supply change

1.4 INSTABILITY OF VENTILATED CAVITIES

Arising the self-induced oscillations of the ventilated cavities [6, 7] is interesting unsteady phenomenon. If too many gas is supplied into the cavity, then it can become unstable. In this case waves arise on the cavity surface, it pulsates along the its length and width, the gas-leakage from the cavity is realized by separation of great cavity portions (air pockets). A photograph of pulsating axisymmetric cavity is presented in Fig. 6 (Yu.F.Zhuravlev).

Theoretically, this phenomenon was explained by E.V.Paryshev [8, 9] on the basis of both the G.V.Logvinovich independence principle and the equation of the mass of gas in the cavity balance.

1.5 CAVITIES AFTER THE WATER ENTRY FROM THE ATMOSPHERE

The air cavity forming after water entry of bodies from the atmosphere, closes on the depth or at the water surface depending on the initial conditions [10]. The cavity pressure is lower than atmospheric one at the cavity closure time. During further immersion of the body, the cavity fast decreases because of both the static pressure growth and the loss of the air entrapped from the atmosphere.

The unsteady process of the depth cavity closure is well described by the approximated mathematical model based on the independence principle [11].

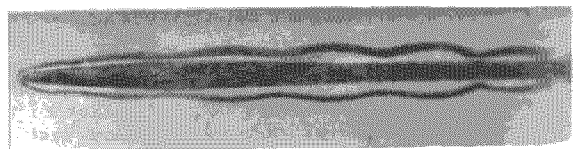

Fig. 6. Pulsating axisymmetric cavity

We have investigated experimentally the interesting phenomenon of wave-shaped deformation of the cavities forming after vertical water entry of bodies with velocity about 10 m/sec [12] (Fig. 7). We showed that cause of this phenomenon consists in excitation of one of fundamental frequencies of the cavity filled by air entrapped from the atmosphere.

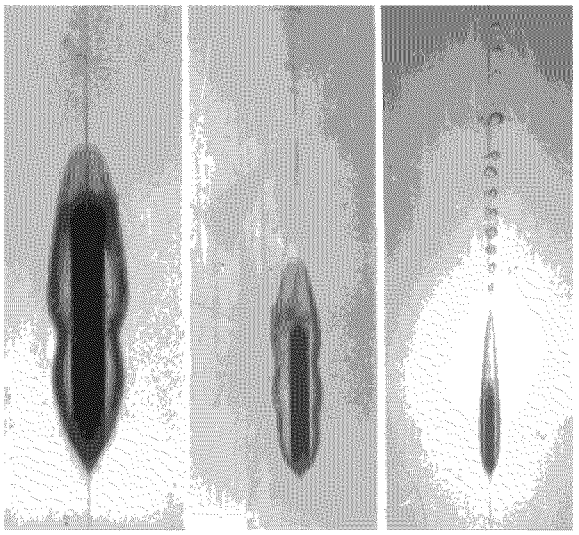

Fig. 7. Cavities after water entry from the atmosphere

2. Mathematical model and calculation algorithm

We use the approximate mathematical model based on the G.V.Logvinovich independence principle of the cavity section expansion for computer simulation of all the mentioned unsteady processes. The mathematical model includes the following equations:

1) The equation of expansion of the unsteady cavity section [13]:

$$\frac{\partial^2 S(\tau,t)}{\partial t^2} = -\frac{k_1 \Delta p(\tau,t)}{\rho}, \quad x(t) - l(t) \le \xi \le x(t), \qquad S(\tau,\tau) = \frac{\pi D_n^2}{4}, \qquad \frac{\partial S(\tau,\tau)}{\partial t} = \frac{k_1 A}{4} D_n V \sqrt{c_x}, \qquad (3)$$

where $\Delta p(\tau,t) = p_\infty(\xi) + p_1(t) - p_c(t)$. Here, $\tau \le t$ is time of section ξ creation; $x(t)$ is the current absolute x-coordinate of the cavitator; $p_1(t)$ is the perturbation of the ambient pressure; $l(t)$ is the cavity length; c_x is the cavitation drag coefficient; $k_1 = 4\pi / A^2$; $A \approx 2$ is the empirical constant. The hydrostatic pressure p_∞ can vary from one section to another when the body moves with the variable depth in ponderable fluid.

2) The equation of the mass of gas in the cavity balance when the gas expands by the isothermal law [8]:

$$\frac{d}{dt}[\overline{p}_c(t)\, Q(t)] = \beta [\dot{q}_{in} - \dot{q}_{out}(t)], \qquad (4)$$

where $\overline{p}_c(t) = p_c(t)/\sigma_0$; σ_0 is the initial cavitation number; Q is the cavity volume; $\dot{q}_{in}$ and $\dot{q}_{out}(t)$ are volumetric rates of air-supply to the cavity and air-leakage from the cavity, respectively, referred to p_∞. We assume that the cavity pressure $p_c(t)$ changes synchronously along the cavity length.

3) The equation of rectilinear motion of the supercavitating model:

$$m\frac{dU}{dt} = \sum F, \qquad (5)$$

where m is the model mass; $U(x,t)$ is the model speed; $\sum F$ is a sum of acting forces (cavitation drag, propeller thrust, gravity when vertical motion etc.). In problems on the supercavitating model dynamics, we use a complete set of the dynamic equation of axisymmetric model [14].

This mathematical model may be applied, strictly speaking, when the parameters change not very fast. In the case of oscillation, we have estimation for dimensionless angular frequency $k << 2\pi a / V_\infty$, where a is the sound speed in the gas filling the cavity. It follows from the assumption that the cavity pressure $p_c(t)$ changes synchronously along the cavity length.

We have developed a "fast" numerical algorithm and a number of computer codes on the basis of the Eqs. (3), (4) and (5). That codes allow to reproduce the unsteady supercavitation processes of the mentioned types on a computer screen [2, 15, 16]. Examples of the computer simulation are given below.

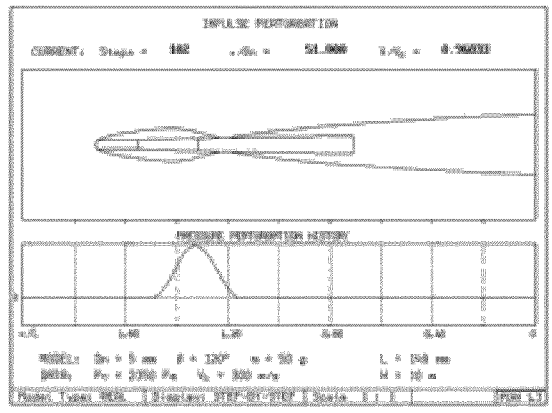

Fig. 8. Result of the PCAV code operation: cavity reaction on the water pressure impulse

3. Cavity deformation under action of the external pressure perturbation

The PCAV code (PerturbedCavity) is intended for computer simulation of supercavity deformation under action of the ambient pressure perturbations in water.

Fig. 8 presents the computer simulation of action of the external pressure impulse imitating the underwater explosion. In this case the cavity pinch occurs when the pressure impulse amplitude is enough. It qualitatively corresponds to the experimental shooting in Fig. 4.

In Fig. 9, a result of computer simulation of the supercavity formation after high-speed water entry through the solid wall is shown. The extra pressure impulse shape $p_1(t)$ in Eq. (3) was evaluated by numerical solving the problem on water penetration of a solid body of revolution. In each time its shape coincides with the cavity shape ("principle of freezing the free boundaries") . The model contour is plotted by thin lines, the cavity contour is plotted by bold lines. The cavity contour at absence of the pressure perturbation is shown by dashed line for comparison. In this case the pressure impulse arising at the water entry of the model results in local pinch of the cavity as well. A comparison with the Fig. 1 shows qualitatively agreement of the calculation and experiment.

The same kind of deformation of the cavity occurs at computer simulation of water entry of the model from within an expanding gas bubble (Fig. 10). In this case the pressure in the fluid may be computed exactly. The model velocity is assumed to be much more than the bubble expansion velocity. The pressure in the cavity is equal to the pressure in the bubble for the starting penetration period.

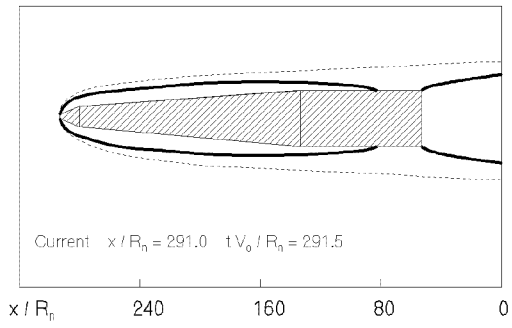

Fig. 9. Result of PCAV code operation: high-speed water entry through a wall

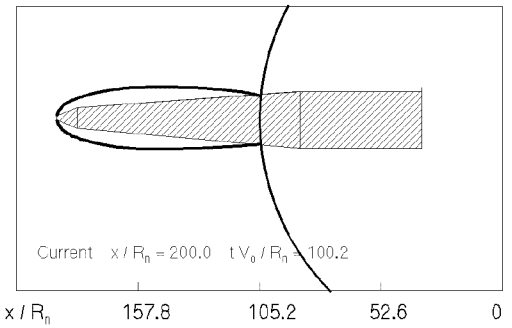

Fig. 10. Result of PCAV code operation: water entry from within an expanding gas bubble

4. Dynamic properties of gas–filled super-cavities

We describe briefly a procedure of the stability analysis and calculation of self-induced oscillation of the axisymmetric gas-filled cavities according to the works [8, 9, 14].

We make dimensionless the Eq. (3) using the initial cavity length l_0 and the velocity V_∞ as scales:

$$\frac{\partial^2 S(\tau,t)}{\partial t^2} = -\frac{k_1 \sigma(t)}{2}, \qquad t - l(t) \le \tau \le t. \tag{6}$$

We consider for simplicity that the cavitator is negligibly small compared to the cavity:

$$S(t,t) = S(t - l(t),t) \to 0, \tag{7}$$

Twice integrating the Eq. (6) with taking account of (7) and using the Dirichlet formula for interchanging integrals, we obtain:

$$S(\tau,t) = \frac{k_1 \sigma_0}{4}\left[t - \tau - 2\int_\tau^t (t-u)\overline{\sigma}(u)du, \right] \tag{8}$$

where $\overline{\sigma}(t) = \sigma(t)/\sigma_0$. Substituting (8) into the cavity closure condition (7), we obtain the equation connecting two unknown functions $\overline{\sigma}(t)$ and $l(t)$:

$$l(t) = 2\int_{t-l(t)}^{t} (t-u)\,\overline{\sigma}(u)du\,. \tag{9}$$

The dimensionless equation of the mass of gas in the cavity balance (4) has the form:

$$\frac{d}{dt}[(\beta - \overline{\sigma}(t))Q(t)] = \beta[\dot{q}_{in} - \dot{q}_{out}(t)]. \tag{10}$$

We calculate the cavity volume, integrating the Eq. (8) along the cavity length and using again the Dirichlet formula:

$$Q(t) = \frac{k_1 \sigma_0}{4}\left[-\frac{l^2(t)}{2} + \int_{t-l(t)}^{t} (t-u)^2\,\overline{\sigma}(u)du \right].$$

The work [3] presents the empirical law of the air-supply for steady axisymmetric cavities when effect of gravity is weak:

$$\dot{q}_{in} = \gamma V_\infty S_c \left(\frac{\sigma_v}{\sigma_0} - 1 \right), \qquad \gamma \approx 0.01 \div 0.02,$$

where $S_c = \pi D_c^2 / 4$ is the cavity mid-section area. We have for the considered processes $p_v << p_\infty$. For the weakly perturbed unsteady cavities, we accept the quasistationary law of the gas-leakage of the same structure [8]:

$$\dot{q}_{out}(t) = \gamma S_c(t) \left(\frac{\beta}{\overline{\sigma}(t)} - 1 \right). \tag{11}$$

The values $\beta = 1$, $\overline{\sigma} \equiv 1$ correspond to the natural vapor supercavity. In this case the Eq. (10) is satisfied identically.

4.1 INSTABILITY OF AXISYMMETRIC VENTILATED CAVITIES

A set of the Eqs. (9) and (10) is related to the class of dynamic system with distributed lag [17]. It has the only stationary point $\overline{\sigma} = 1$, $l = 1$. We investigate it on stability relatively to small oscillations. Representing the unknown functions in the form:

$$\overline{\sigma}(t) = 1 + \varepsilon \sigma_1(t), \quad l(t) = 1 + \varepsilon l_1(t), \quad \varepsilon \approx o(1),$$

and linearizing the equations and excepting $l_1(t)$, we obtain the uniform equation with respect to $\sigma_1(t)$:

$$\dot{\sigma}_1(t) - 12(\beta - 1) \int_0^1 \theta(\theta - 1) \dot{\sigma}_1(t - \theta) d\theta + \frac{3}{2} \gamma \beta (2\beta - 1) \sigma_1(t) = 0. \tag{12}$$

Following to a usual procedure of investigation of solutions of the equations on stability with respect to small oscillations, we do the substitution in the Eq. (12)

$$\sigma_1(t) = a e^{\mu t}, \qquad \mu = \lambda + jk$$

and obtain its characteristic equation:

$$\mu^3 + \frac{3}{2} \gamma \beta (2\beta - 1) \mu^2 + 12(\beta - 1)[\mu(e^{-\mu} + 1) + 2(e^{-\mu} - 1)] = 0. \tag{13}$$

Here, k is the reduced oscillation frequency, $k = \omega l_0 / V_\infty$; λ is the oscillation increment. The oscillation with frequency k damps when $\lambda < 0$ and increases indefinitely when $\lambda > 0$.

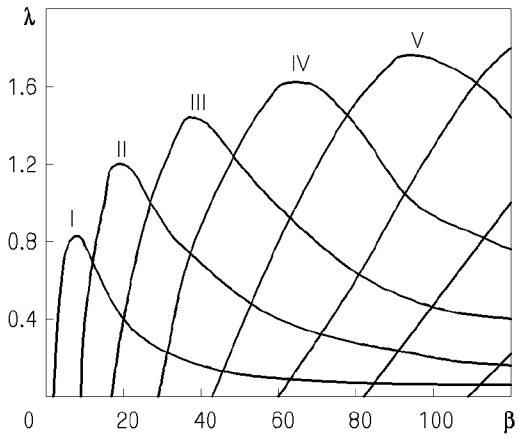

Fig. 11. Real part of the characteristic Eq. (13) roots

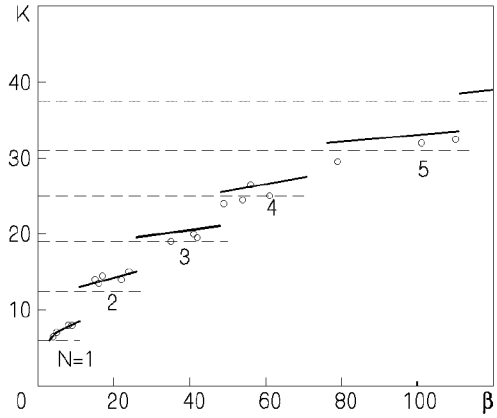

Fig. 12. Modes of the axisymmetric cavity pulsation

In the first case the solution of the Eq. (12) is asymptotically stable, in the second case it is unstable. The frequency k which corresponds to the increment value $\lambda = 0$ is called the fundamental frequency of the dynamic system.

The Eq. (13) contains two physical parameters γ and β. When $\gamma \neq 0$, it has the double root $\mu = 0$ which transforms into threefold one when $\gamma = 0$. It is not difficult to make sure by direct checking that the corresponding secular solutions [17] do not satisfy the Eq. (12). When $\gamma = 0$, the Eq. (13) has a series of the pure imaginary roots, i.e. the fundamental frequencies:

$$k_n = 2\pi n, \qquad \beta_n = 1 + \frac{(\pi n)^2}{6}, \qquad n = 1, 2, \ldots \tag{14}$$

Fig. 11 presents graphs of distribution of the real part of the Eq. (13) roots when $\gamma = 0$. When $\beta \to \infty$, the curves asymptotically approaches to the x-axis. We suppose that the frequency corresponding to the maximal linear increment λ "survives" among severe fundamental frequencies for the given value of β. In a result we obtain estimation of the mode boundaries of the cavity self-induced oscillation (solid lines in Fig. 12).

Thus, when $\gamma = 0$, the cavity is asymptotically stable when $1 \leq \beta < 2.645$ and unstable when $\beta > 2.645$. The value $\gamma = 0$ corresponds to the case when the mass of gas in the cavity is constant. An analysis of the characteristic Eq. (13) shows that it is possible to point a finite interval of changing the value β for each $0 < \gamma < 0.08$. Outside this interval, the zero solution of the Eq. (12) is asymptotically stable, and within this interval it is unstable (Fig. 13). Within the instability zone and when $\gamma \neq 0$, the characteristic equation has the finite number of pure imaginary roots. Their quantity decreases with increasing γ. When $\gamma > 0.08$, roots are absent in general, i.e. the cavity is asymptotically stable for any β.

The established behaviour of effect of the gas-leakage variability on the cavity stability qualitatively explains the experimental fact that the cavity pulsation ceases when the gas-supply becomes very great. So, in the experiments [6, 7], five waves on the pulsating cavities ($N = 5$) have been observed at most.

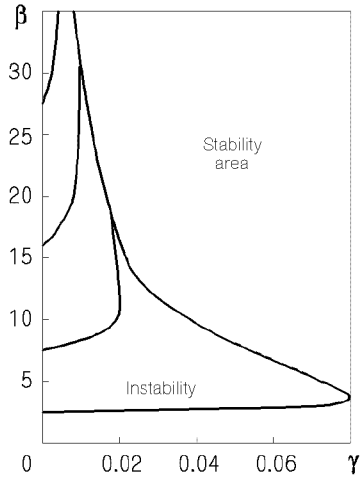

Fig. 13. Influence of the parameter γ

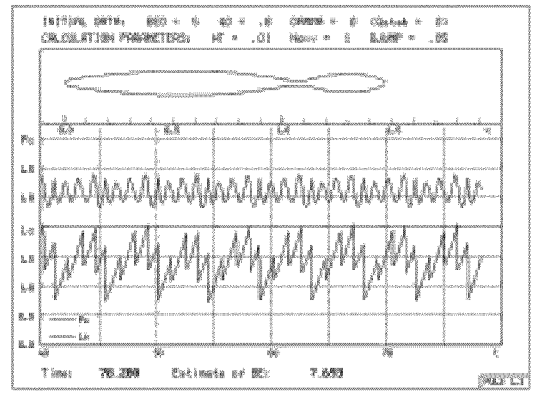

Fig. 14. Result of the PULSE code operation (mode II)

4.2 SELF-INDUCED OSCILLATION OF VENTILATED CAVITIES

For the first time, calculation of self-induced oscillations developing after the stability loss of the ventilated cavity was performed by E.V.Paryshev [9]. We have developed the computer code PULSE that allows to reproduce the cavity pulsation on a computer screen "in real run-time" and to carry out its Fourier analysis [15].

Calculation showed that pulsation arises in the dynamic system described by Eqs. (3) and (4) when the parameter β is in the linear instability zone ($\beta > \beta_1 = 2.645$) . The oscillation develops until the establishment of the periodic or the quasiperiodic pulsation with discontinuous dependence l(t). Fig. 14 shows a view of the computer screen during run-time of the code PULSE. Fig. 15 shows evolution of spectrum of the cavity pressure when the bifurcation parameter $q_0 = \beta_0 \dot{q}_{in}$ increases. Increasing the bifurcation parameter q_0 is accompanied by spasmodic appearance of new frequencies and their linear combinations in the spectrum $\overline{p}_c$. This corresponds to passage up to higher modes of the cavity pulsation. The spectrum $\overline{p}_c$ becomes complicated within each mode, remaining the line one. In this case the basic harmonic changes weakly.

The same behaviour of unsteady ventilated cavities is observed experimentally [6, 7].

Fig. 16 shows spectra of the cavity pressure oscillation under action of forced oscillation of the external pressure $\overline{p}_1(t) = \kappa \sin k_f t$ (q_0 = 0.8, κ = 0.1). The corresponding spectrum $\overline{p}_c(t)$ when the external perturbation is absent is given in Fig. 15, a. We have the modulation when $\tilde{k}_f << \tilde{k}_I$ (a), the synchronization when $\tilde{k}_f \approx \tilde{k}_I$ (b) or the "chaotization" when $\tilde{k}_f > \tilde{k}_I$ (c) of the periodic mode I in depending on a ratio of the forcing frequency $\tilde{k}_f$ to the cavity oscillation frequency $\tilde{k}_I$ (they both are referred to the average cavity length l_m).

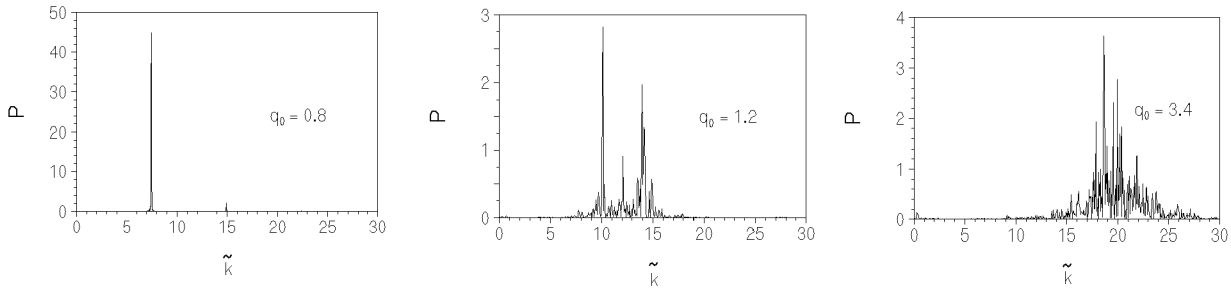

Fig. 15. Power spectral density of $p_c(t)$ at the self-induced oscillation

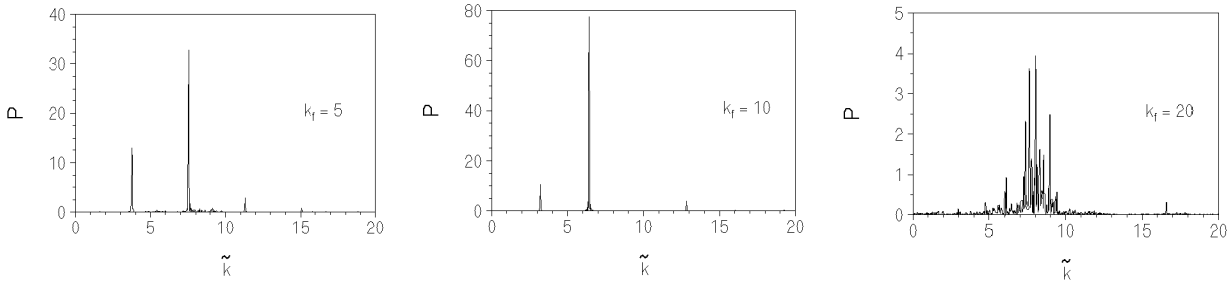

Fig. 16. Power spectral density of $p_c(t)$ at the forced oscillation

4.3 WAVE FORMATION ON THE CAVITY AFTER WATER ENTRY FROM THE ATMOSPHERE

We already spoke of the wave formation phenomenon on the cavities forming at vertical water entry of bodies through the free surface from the atmosphere with the velocities 5 ÷ 10 m/sec [12].

It was established experimentally [18] that the free water surface influence on the drag coefficient c_x and on the cavity shape near the cavitator propagates only on the depth of 1.5 ÷ 2 cavitator diameters. This result gives background to use the approximate Eq. (3) for computer simulation of penetration of the bodies through the free surface into water.

To explain this phenomenon we have applied results of the linear theory of gas-filled supercavity instability. We showed that its cause consists in excitation of one of the fundamental frequencies of the cavity filled by air entrapped from the atmosphere. In the case of enough high both the body mass and the initial Froude number Fr_0, we obtain a priori estimation of the wave number N on the cavity:

$$N = \left[\frac{1}{\pi} \sqrt{\frac{2Eu_0 Fr_0}{B}} \right], \quad B = \sqrt{\sqrt{c_x}}, \tag{15}$$

where $Eu_0 = 2p_{atm} / \rho V_0^2$ is the Euler number. The estimation (15) is in good agreement with the experimental data.

The calculation model of that process after the cavity depth closure includes three Eqs. (3), (4) and (5). Their solution is sought numerically by iteration process for each time step. Fig. 17 presents graphs of both the cavity length and the cavity pressure as functions of the cavitator immersion x. The graph of the dependence $l(x)$ which was calculated without taking account of the air elasticity is plotted by a dashed line. A comparison of the calculated shape and the experimental shape of the cavity for three sequential times is given in Fig. 18.

The obtained good agreement of the calculation and experiment for such complicated unsteady process confirms adequacy of the accepted approximate mathematical model of the unsteady axially symmetric supercavity.

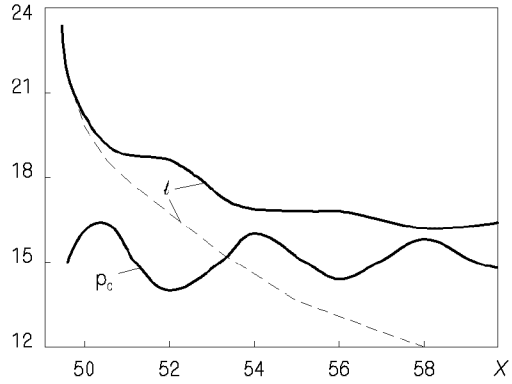

Fig. 17. Cavity history after vertical water entry: graphs of $\overline{p}_c(t)$ and $l(t)$

5. Control of the ventilated cavities

A problem of control of the ventilated cavity is the problem of maintaining the cavity dimensions or of varying the cavity dimensions according to the given law by regulating the gas-supply into the cavity. Examples of the typical control problems are:

1) How should the gas-supply rate be varied for maintenance of the invariable cavity if the motion velocity and/or the motion depth change?

2) What is the law governing the cavity collapse if the gas-supply to the cavity is rapidly stopped?

The difficulty of the problem on the ventilated cavity control is caused by non-linearity and non-monotonicity of the dependence $\dot{q}_{in}(t) = f(\sigma)$ [3, 4] and by the multiparametric nature and lack of knowledge of the gas-leakage laws as well.

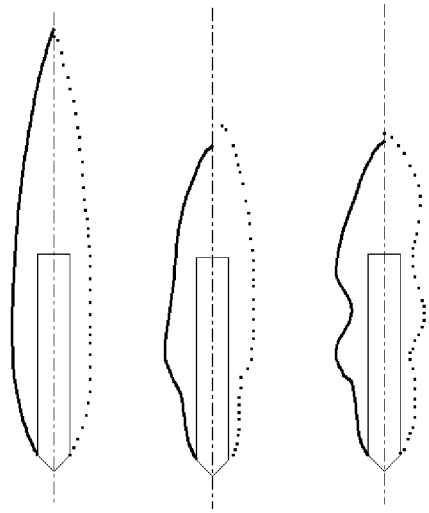

Fig. 18. Cavity history after vertical water entry: ------ - calculation, - - - - experiment

We have developed the computer code ACAV (ArtificialCavitation) for computer simulation of unsteady processes at the ventilated cavity control. It allows to use any laws of varying the air-supply, the air-leakage and the model velocity as well.

Fig. 19 shows a view of the computer screen during run-time of the code ACAV. In this case, the model quasi-stationary law of the gas-leakage from the cavity was used:

$$\dot{q}_{out}(t) = \frac{2 \cdot 10^{-5}}{\sigma^4(t)}. \tag{16}$$

It corresponds to the second type of the gas-leakage by vortex tubes.

In the code ACAV, the set of the Eqs. (3) and (4) is integrated with the constant step with respect to dimensionless longitudinal variable x. During computation in Fig. 19, the gas-supply rate into the cavity increases in 2.4 times on the distance $\Delta x = 0.5$, then remains constant on the distance $\Delta x = 1.0$ and than decreases to its initial value. The calculation gives a characteristic lagging reaction of the cavity on the changing the rate which is observed in experiments.

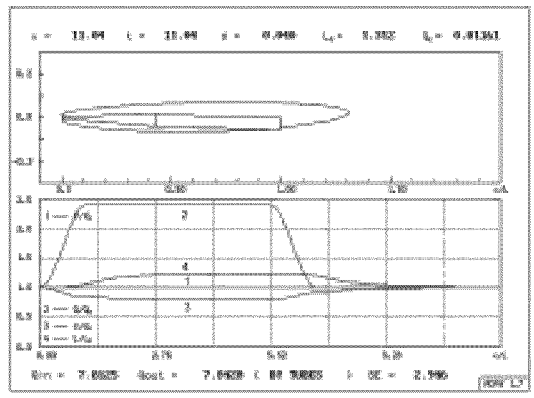

Fig. 19. Result of the ACAV code operation

5.1 CAVITY REACTION ON CHANGING THE GAS–SUPPLY RATE

Firstly we consider peculiarities of the ventilated cavity reaction on changing the air-supply rate $\dot{q}_{in}(t)$ when the model velocity is constant: $V_0 = \text{const}$. Here we present results of computer simulation for two types of changing the supply: 1) impulse increase of the air-supply; 2) rapid single decrease of the air-supply.

At the calculation, we used the following parameters of the model: the disk cavitator with diameter $D_n = 200$ mm; the cavitator slope angle $\delta = 10°$; the model tail diameter $D_s = 350$ mm; the model length $L = 7$ m. Also, we used the following common starting values of the parameters: $V_0 = 100$ m/c; the motion depth $H = 5$ m; $\sigma_0 = 0.04$; the model pitch angle $\psi = 2°$. In this case the starting cavity length is $L_c = 9.06$ m when the balanced air-supply coefficient is $\dot{q}_0 = 7.813$.

In Figs. 20, 21, the following legends are used for marking the curves: $1 - \dot{q}(t)$; $2 - \sigma(t)$; $3 - l(t)$; $4 - V(t)$.

Fig. 20,a demonstrates a calculation result of the cavity reaction on the impulse increase of the air-supply. One can see that the cavity length reacts on the rate change with greater lagging than the cavity pressure. All the cavity parameters return to their starting values after the impulse end.

A calculation result of the cavity reaction on the rapid decreasing the air-supply is shown in Fig. 20, b. In this case the cavity does a number damped oscillations (a transient process), then establishes new balanced values of the parameters: L_c = 6.09 m; σ =0.06 m; $\dot{q}_{in}$ = 1.563.

A cause of the transient process is the elasticity effect of the gas filling the cavity when the cavity volume rapidly decreases. We note that self-induced oscillations of the cavity may arise for other starting parameters (smaller values of V_0 and higher values of σ_0).

5.2 CAVITY REACTION ON CHANGING THE MODEL VELOCITY

Now we consider peculiarities of the ventilated cavity reaction on varying the model velocity V when the gas-supply rate is constant: $\dot{q}_{in}$ = const.

The calculation result of the ventilated cavity reaction on increasing the model velocity is shown in Fig. 21, a. One can see that the cavity length increases very significantly (in quasi-stationary approximation it is proportional to the velocity square), but the cavity pressure changes weakly. It is typical for this case that the unsteady cavity length considerably exceeds the new balanced level L_c = 13.0 m.

The calculation result of the ventilated cavity reaction on decreasing the model velocity is shown in Fig. 20, b. A comparison with Fig. 20, a shows a difference from the cavity reaction on the air-supply decrease that consists in absence of the transient process. The new balanced cavity length is L_c=2.34m.

We can investigate with the ACAV code the ventilated supercavity behavior when the model motion velocity $V(t)$ and the air-rate into the cavity $\dot{q}_{in}(t)$ change simultaneous. In this case we can try to obtain answers for two practically important questions:

1) May we accelerate the cavity development on the accelerating phase of the body motion by means of increasing the gas-supply into the cavity ?

2) How long may we maintain the cavity with given dimension by means of increasing the gas-supply when the body velocity decreases?

The computer simulation allows to conclude that the air-supply increase when the model velocity increase does not result in considerable decrease of time of the cavity development to the balanced length at the accepted law of the gas-leakage from the cavity (16). This conclusion is valid in the case when the model velocity is already high, and the supercavity already exists.

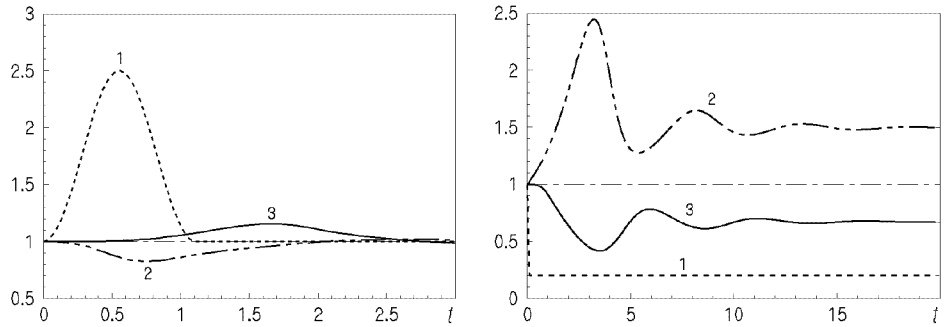

a *b*

Fig. 20. Cavity reaction on varying the gas-supply rate
a – impulse increasing the gas-supply rate; *b* – rapid decreasing the gas-supply rate

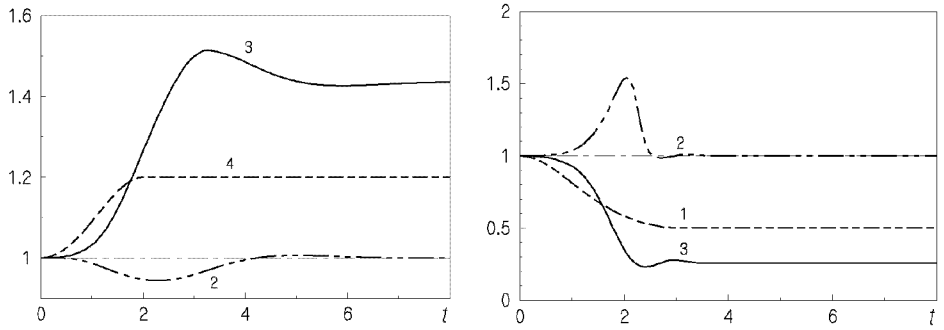

Fig. 21. Cavity reaction on varying the model velocity: *a* – increasing the velocity; *b* – decreasing the velocity

5.3 INFLUENCE OF THE PARAMETER β AND THE GAS–LEAKAGE TYPE

Considerable difference between the natural vapor and ventilated supercavities appears in the case of the unsteady flow. In this case the parameter β is of importance that characterizes effect of elasticity of the gas filling the cavity.

A dependence of changing the cavity length L_c on the parameter β_0 is shown in Fig. 22. The calculation was performed with the code ACAV when D_n = 200 mm. The free cavity closure and the gas-leakage law (16) were accepted at calculation. The cavitation number was constant and equal to σ = 0.06. The starting cavity dimensions were: L_c = 6.04 m, D_c = 0.74 m.

The model velocity firstly increases on 50% along the distance 10 m, then remains constant along the distance 100 m, next decreases to its starting value. A graph of the model velocity variation is shown by dotted line.

The curve 1 corresponds to the natural cavitation regime $\beta \equiv 1$. In this case the starting model velocity was V_0 = 69.5 m/sec.

In the artificial cavitation regime, changing the parameter β at the constant σ is attained by changing the starting model velocity V_0. We used the data:

curve 2 – V_0 = 50 m/sec, β_0 = 1.96;

curve 3 – V_0 = 30 m/sec, β_0 = 5.45.

The presented graphs visually demonstrate increasing the effect of the gas elasticity with increasing the parameter β. In the last case (the curve 3) undamped self-induced oscillations of the cavity develop according to the theory of instability of gas-filled cavities. In this case the starting value of the parameter is β = 7.358 > 2.645, i.e. the cavity is unstable according to (14).

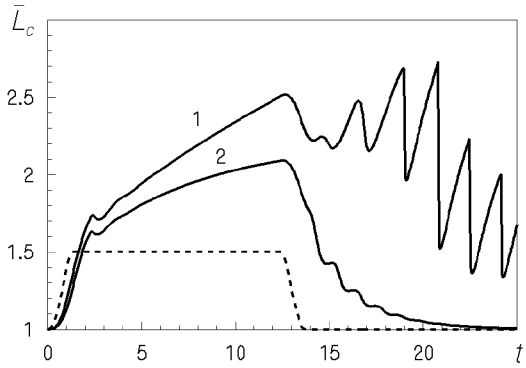

Fig. 22. Influence of the parameter β the cavity behaviour

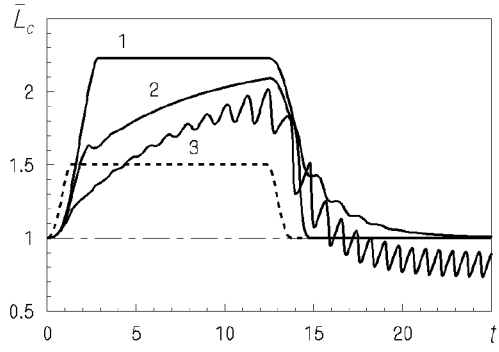

Fig. 23. Cavity behaviour at various on types of the gas-leakage

In Fig. 23, the dependence $L_c(t)$ which has been calculated for different laws of the gas-leakage from the cavity is shown. The model velocity changed in the same way as in Fig. 22. In calculation we assumed that the leakage coefficient is a single-valued function of the cavity pressure: $\overline{Q} = \overline{Q}(p_c)$. Different curves in the figure correspond to the following gas-leakage laws:

curve 1 – the 1st type of the portion gas-leakage ;

curve 2 – the 2nd type of the gas-leakage by vortex tubes, the formula (16).

For the 1st type of the gas-leakage we used a function obtained by the experimental data [4] approximation:

$$\overline{Q} = \frac{5\sigma}{100\sigma^2 + 1}. \tag{17}$$

Considerable difference of the cavity behaviour confirms importance of observance of the gas-leakage type similarity at both the physical modeling and the computer simulation of unsteady ventilated cavities.

Presence of the model body within the cavity decreases active volume of the cavity filled by gas. This does not influence on the cavity dimension in the case of the steady flow at the cavity free closure (if we do not take into account the possible interaction between the model and the reentrant jet). In the non-stationary case we have quite another situation. It is necessary to take into account decreasing the active cavity volume in the equation of the mass of gas balance (4). This causes to changing the dynamic cavity behaviour.

6. Comparison of unsteady behaviour of 2-D and axisymmetric supercavities

It follows from said before that the approximate equation of the cavity section expansion (3) based on the G.V.Logvinovich independence principle gives an effective (and usually unique) method of calculation of the unsteady supercavitation flows.

The independence principle is approximate one, and its verification has great methodological significance. The experimental tests justify its validity in wide range of the parameters [2].

The Eq. (3) well describes the mean part of the supercavity, i.e. it is in essence linear one. A comparison of calculation results of the unsteady cavity shape by the Eq. (3) with the theoretical solutions, which are obtained in the linearized theory of two-dimensional super-cavitation flows [19–22], is of interest.

We use the solutions of two 2-D problems for comparison:

1) the problem on instability of the 2-D gas-filled supercavity;

2) the problem on evolution of the 2-D supercavity at the forced oscillations.

The linear theory application to this problems is correct, because the ventilated cavities always have very great aspect ratio at the time of the stability loss [6, 7].

6.1 MATHEMATICAL MODELS OF THE 2-D UNSTEADY SUPERCAVITY

Two alternative approaches are applied to solve the steady and non-stationary 2-D linearized problems on the supercavitation flow [23, 24]:

1) the method of boundary value problems for analytical functions;

2) the method of integral equations (a variant of the method of boundary integral equations).

The first method gives a solution in the form of quadratures. It is convenient for analytical investigation of stability of the 2-D gas-filled cavity .

The second method is more convenient for numerical calculations when the cavity length is variable. It is easy generalized for the bounded flows, for the super-cavitating hydrofoils in hydrodynamic cascades and for the hydrofoils of finite span as well.

6.1.1 Method of boundary value problem for analytical functions

We construct firstly a solution of the linear unsteady problem by the 1st M.Tulin's scheme (Fig. 24). For simplicity, we consider so called "pure" supercavity, i.e. we assume that the cavitator dimension is negligibly small compared to the cavity.

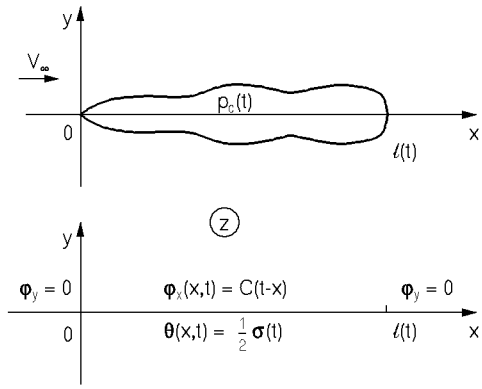

Fig. 24. Two-dimensional "pure" unsteady supercavity
by the 1st M.Tulin's scheme

All the variables are assumed to be dimensionless. The initial cavity length l_0 and the velocity V_∞ are accepted as the length scale and the velocity scale, respectively. We consider two analytical functions:

the complex velocity $\overline{V}(z,t)=\varphi_x-i\varphi_y$ and the complex acceleration potential $\Phi(z,t)=\theta+i\chi$. We have:

$$\theta(x,y,t)=\frac{p_\infty-p(x,y,t)}{\rho}=N\varphi(x,y,t),\quad N=\frac{\partial}{\partial t}+\frac{\partial}{\partial x}. \tag{18}$$

On the x-axis, the components of $\Phi(z,t)$ and $\overline{V}(z,t)$ are connected by relations:

$$\theta(x,t)=\theta(-\infty,t)+\varphi_x(x,t)+\int_{-\infty}^{x}\varphi_{xt}(s,t)ds, \tag{19}$$

$$\chi(x,t)=\chi(-\infty,t)-\varphi_y(x,t)-\int_{-\infty}^{x}\varphi_{yt}(s,t)ds. \tag{20}$$

The cavity pressure $p_c(t)$ must be constant at each time along the cavity length. Thus, we have the boundary condition for the acceleration potential:

$$\theta(x,t)=\frac{\sigma(t)}{2},\qquad 0<x<l(t). \tag{21}$$

The cavity length $l(t)$ is an unknown time function. The cavity pressure p_c and, therefore, the cavitation number σ are unknown time functions in the case of the gas-filled supercavity.

Differentiating the Eq. (21) with respect to x and applying the inverse operator N^{-1}, we obtain the boundary condition for perturbed horizontal velocity:

$$\varphi_x(x,t)=C(t-x),\qquad 0<x<l(t),$$

where $C(t)$ is an arbitrary time function. Out the interval $[0,l(t)]$ we have $\varphi_y=0$ because of the flow symmetry and absence of sources in the cavity wake.

According to the 1st M.Tulin scheme, the "pure" super-cavity has a shape of ellipse in the stationary case:

$$F(x)/\sigma_0=\frac{1}{2}\sqrt{x(l_0-x)},\qquad 0\le x\le l_0.$$

In the points $z=0$, $z=l_0$, the complex velocity has singularities of the order $O\left(x^{-\frac{1}{2}}\right)$ and $O\left((l_0-x)^{-\frac{1}{2}}\right)$. We assume that the solution must have singularities of the same order for unsteady supercavity in each time on the ends of the interval $[0,l(t)]$.

Thus, we have the mixed boundary value problem for the function $\overline{V}(z,t)$ in the upper half-plane $\operatorname{Im} z>0$:

$$\varphi_y=0,\quad at\quad -\infty<x<0,\quad \varphi_x=C(t),\quad at\quad 0<x<l(t),\quad \varphi_y=0,\quad at\quad l(t)<x<\infty. \tag{22}$$

The solution of this problem in the class of functions unlimited on the ends of interval $[0,l(t)]$ is given by Keldysh-Sedov formula [25]:

$$\overline{V}(z,t)=\frac{1}{4}\sqrt{\frac{l}{z(z-1)}}+\frac{1}{\pi}\sqrt{\frac{z}{z-l}}\int_0^l C(t-s)\sqrt{\frac{l-s}{s}}\frac{ds}{s-z}. \tag{23}$$

Here and later, functions $\overline{V}$ and C are related to σ_0.

The solution (23) gives a logarithmic singularity of the pressure at infinity. It is caused by variability of the 2-D closed cavity in unbounded fluid. This methodological paradox disappears when the free boundary is in the flow.

To determine the cavity shape $F(x,t)$ we use the linearized kinematic condition on the cavity boundary [24]

$$\varphi_y(x,t) = N F(x,t), \qquad 0 < x < l(t). \tag{24}$$

From here, using the relation (20) and the Dirichlet formula for interchanging integrals, we obtain the expression for both the shape and the volume of the unsteady symmetric cavity:

$$F(x,t) = \int_0^x (x-s)\chi_t(s,t-x+s)ds - \int_0^x \chi(s,t-x+s)ds, \tag{25}$$

$$Q(t) = -2\int_0^l (l-s)\chi(s,t-l+s)ds, \tag{26}$$

where

$$\chi(x,t) = -\frac{1}{4}\sqrt{\frac{l}{x(l-x)}} + \left(\frac{\overline{\sigma}}{2} + \frac{\dot{q}}{\pi}\ln\frac{2}{\sqrt{l}}\right)\sqrt{\frac{x}{l-x}} - \frac{\dot{q}}{\pi}\arctan\sqrt{\frac{x}{l-x}},$$

$$q(t) = 2\pi\left[\frac{\sqrt{l}}{4} - \frac{1}{\pi}\int_0^l C(t-s)\sqrt{\frac{l-s}{s}}\,ds\right].$$

It is necessary to fulfill the natural boundary condition (21) to eliminate the auxiliary function $C(t)$. Calculating the acceleration potential on the interval $[0, l(t)]$ by the formula (19), we obtain the equation:

$$\frac{\dot{l}}{4\sqrt{l}} + \frac{1-\dot{l}}{\pi}\int_0^l \frac{C(t-s)ds}{\sqrt{s(l-s)}} - \frac{\dot{q}}{\pi}\ln\frac{2}{\sqrt{l}} = \frac{\overline{\sigma}}{2}. \tag{27}$$

The constructed solution of the unsteady problem (23), (27) contains two unknown time functions $\overline{\sigma}(t)$ and $l(t)$. To determinate them we use the condition of the cavity to be close in each time:

$$\int_0^l (l-s)\chi_t(s,t-l+s)ds - \int_0^l \chi(s,t-l+s)ds = 0 \tag{28}$$

and equation of the mass of gas in the cavity balance (4).

In the case of steady flow, the solution (23) has the form:

$$\overline{V}(z) = \frac{1}{2}\left[\frac{l_0}{2\sqrt{z(z-l_0)}} + 1 - \sqrt{\frac{z}{z-l_0}}\right]. \tag{29}$$

We note that the parameters σ_0 and l_0 are independent for stationary "pure" supercavity.

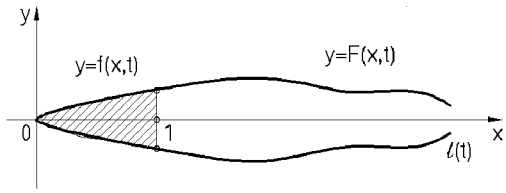

Fig. 25. Unsteady flow around supercavitating wedge

6.1.2. Method of integral equations

Now we construct the solution by the method of integral equations for the unsteady problem on supercavitation flow around a thin symmetric wedge with unit length (Fig. 25). Let the unsteady perturbation of the flow caused by deformation of the wedge sides so that a shape of the wedge is given by the function:

$$y = \pm f(x,t) \sim O(\varepsilon), \quad 0 < x < 1, \tag{30}$$

where ε is the small parameter. In this case the kinematic boundary condition on the upper side of the wedge is added to the boundary conditions (22), (24):

$$\varphi_y = N f(x,t), \quad 0 < x < 1; \qquad y = +0\ . \tag{31}$$

Because of the flow symmetry, we can obtain the flow satisfying the boundary conditions (24), (31) when we place a layer of 2-D sources with the linear intensity $q(x,t)$ on the interval $[0, l(t)]$ of the x-axis. At the arbitrary point (x, y) of the flow, the sources induce the total potential:

$$\varphi(x,y,t) = \frac{1}{2\pi} \int_0^{l(t)} q(s,t) \ln \sqrt{(x-s)^2 + y^2}\, ds. \tag{32}$$

The source intensity is equal to a jump of the normal velocity of the fluid φ_y at passage through the x-axis. We have for the flow symmetric about the x-axis:

$$q(s,t) = 2\varphi_y(s,t), \qquad 0 < s < l(t). \tag{33}$$

Applying the linear operator N to the expression (32), we obtain the acceleration potential of unsteady sources distributed along an interval with a variable length:

$$\theta(x,y,t) = \frac{1}{2\pi} \int_0^{l(t)} q(s,t) \frac{x-s}{(x-s)^2 + y^2} ds + \frac{1}{2\pi} \frac{\partial}{\partial t} \int_0^{l(t)} q(s,t) \ln \sqrt{(x-s)^2 + y^2}\, ds. \tag{34}$$

Passing to the limit $y \to 0$ in Eq. (34) and substituting it in the boundary condition (24), we obtain the integro-differential equation

$$\int_0^{l(t)} \frac{q(s,t)ds}{x-s} + \frac{\partial}{\partial t} \int_0^{l(t)} q(s,t) \ln |x-s|\, ds - \pi\sigma(t) = 0\ , \tag{35}$$

where $1 < x < l(t)$. The intensity of the sources distributed along the interval [0, 1] is known:

$$q(x,t) = 2Nf(x,t), \qquad 0 \le x \le 1.$$

Thus, the Eq. (35) may be finally rewritten in the form:

$$\int_1^{l(t)} \frac{q(s,t)ds}{x-s} + \frac{\partial}{\partial t} \int_1^{l(t)} q(s,t) \ln |x-s|\, ds - \pi\sigma(t) = A_1(x,t), \tag{36}$$

where the function $A_1(x,t)$ in the right part is easy calculated for the concrete law of unsteady deformations of the wedge (30):

$$A_1(x,t) = -2 \int_0^1 \frac{Nq(s,t)ds}{x-s} - 2 \int_0^1 N\dot{q}(s,t) \ln |x-s|\, ds. \tag{37}$$

Then, we obtain the equation of the upper cavity boundary from the kinematic condition on the cavity (24) when $1 \le x \le l(t)$:

$$F(x,t) = N^{-1}\varphi_y(x,t) = \frac{1}{2}\int_0^x q(s, t-x+s)ds. \tag{38}$$

Since the cavity length $l(t)$ and the cavitation number $\sigma(t)$ are unknown time functions in the general case, it is necessary to add two relations to the Eq. (36):

1) the condition of solvability of the Newmann's external boundary value problem for the velocity potential

$$\int_0^{l(t)} q(s,t)ds = 0; \tag{39}$$

2) the equation of the mass of gas in the cavity balance (4) for gas-filled cavities. In the case of natural vapor supercavities the Eq. (4) is replaced by the condition $p_c = \text{const}$.

As a result, we obtain a set of three equations to determine the functions $q(x,t)$, $l(t)$ and $\sigma(t)$. It must be integrated with respect to time with the initial conditions

$$q(x,0) = q_0(x), \quad l(0) = l_0, \quad \sigma(0) = \sigma_0. \tag{40}$$

The condition (39) ensures limitation of the pressure at infinity. In the partial case of the steady flow, the Eq. (39) is the cavity closure condition. In the case of the unsteady flow, the cavity is unclosed.

It is necessary to distribute 2-D vortexes with the linear intensity $\gamma(x,t)$ along the projection of the foil on the x-axis [24] together with the sources in the general case of nonsymmetric flow around the supercavitating hydrofoil. This adds one more singular integral equation to the set of equations. Our paper [26] presented results of solving the problem on supercavitating flow around an oscillating hydrofoil near the water surface.

6.2. INSTABILITY OF THE 2-D VENTILATED CAVITY

Using the solution of the equation set (27), (28) and (4), we investigate stability of the "pure" 2-D supercavity in the unbounded flow.

According to the experimental data [6] for the steady plane supercavities, the air-supply rate may be approximated by the linear function (in the dimensional form):

$$\dot{q}_{in} = \gamma b_0 V_\infty \left(1 - \frac{\sigma_0}{\sigma_v}\right), \tag{41}$$

where γ is the empirical coefficient; b_0 is the cavity mid-section. It is valid for the steady "pure" cavity (29) that

$$b_0 = \frac{\sigma_0 l_0}{2}.$$

We assume that when oscillation of the cavity pressure is small, the air-leakage rate depends in quasi-stationary way on $p_c(t)$:

$$\dot{q}_{out}(t) = \gamma b(t) V_\infty \left(1 - \frac{\sigma(t)}{\sigma_v}\right). \tag{42}$$

Passing to the dimensionless variables and using the quasi-stationary dependence $b(\sigma)$, we obtain from the Eq. (4):

$$\frac{d}{dt}[(\beta - \overline{\sigma}(t))Q(t)] = \frac{\gamma}{2}(\beta - \overline{\sigma})\left[1 - \frac{1}{\beta} - \frac{1}{\overline{\sigma}}\left(1 - \frac{\overline{\sigma}}{\beta}\right)\right]. \tag{43}$$

The set of equations (27), (28) and (43) relates to the class of nonlinear autonomous equations with distributed lag of Volterra type. Their properties are similar to properties of ordinary differential equations with a lagging argument [17].

This set has the only stationary point $\overline{\sigma} = 1$, $l = 1$, $C = 0.5$. It corresponds to the steady supercavity (29). We linearize the equations in the stationary point neighbourhood, representing the unknown functions in the form:

$$\overline{\sigma}(t) = 1 + \varepsilon a e^{\mu t}, \qquad l(t) = 1 + \varepsilon b e^{\mu t}, \qquad C(t) = \frac{1}{2} + \varepsilon c e^{\mu t}$$

and saving the only terms of order $O(\varepsilon)$. Here, $\mu = \lambda + jk$, $k = \omega l_0 / V_\infty$ is the reduced frequency of the oscillations; *a, b, c* are constants. In this case the integrals in the equations are expressed by the modified Bessel functions of the 1st kind $I_0(\mu/2)$ and $I_1(\mu/2)$ [27]. As a result, we obtain the set of the linear uniform equations with respect to unknowns *a, b, c*. We do not present it here because its awkwardness. Equating the determinant of the equation set to zero, we obtain the characteristic equation:

$$A[\mu^2(I_0^2 - I_1^2) + 2\mu I_0(2I_0 + I_1) + 2I_0^2] + [\mu A \ln 2 + 4(\beta - 1)][2I_0 I_1 + \mu(I_0 + I_1)(I_0 + 3I_1)] = 0, \tag{44}$$

$$A = 8[\mu Q_0 + \gamma(\beta - 1)]/\pi.$$

where $Q_0 = \pi\sigma_0 l_0^2 / 8$ is the volume of the stationary pure" cavity (29).

We suppose firstly that the mass of gas in the cavity is constant, i.e. $\gamma = 0$. In this case the Eq. (44) contains the only physical parameter β. It is easy to make sure that $\mu = 0$ is the only real root of the Eq. (44). Assuming $\lambda = 0$ and using the relations:

$$I_0\left(\frac{jk}{2}\right) = J_0\left(\frac{k}{2}\right), \qquad I_1\left(\frac{jk}{2}\right) = jJ_1\left(\frac{k}{2}\right),$$

where J_0, J_1 are the Bessel functions of the 1st kind, we establish that the Eq. (44) has two series of alternating pure imaginary roots, i.e. frequencies of the fundamental oscillations $k_n^{(1)}, k_n^{(2)}, \ldots$ They satisfy the equations:

$$J_0\left(\frac{k_n^2}{2}\right) = 0, \qquad kJ_1(J_0^2 + J_1^2) + J_0(J_0^2 - J_1^2) = 0.$$

Corresponding values of the parameter β are:

$$\beta_n^{(1)} = 1 + \frac{2Q_0(3\ln 2 - 1)}{3\pi}k^2, \quad \beta_n^{(2)} = 1 + \frac{2Q_0}{\pi}\left[k^2 \ln 2 - \frac{kJ_0(k/2)}{J_1(k/2)}\right]. \tag{45}$$

A numerical analysis of the complex roots of the Eq. (44) shows that we have $\lambda > 0$ when $k_n^{(1)} < k < k_n^{(2)}$, $n = 1, 2, \ldots$, i.e. oscillation with such frequencies is unstable. A graph of the dependence

of $\lambda(\beta)$ is presented in Fig. 26. A comparison with Fig. 11 shows that the distributions of the characteristic equation roots is qualitatively similar for the dynamic models of both the two-dimensional and the axisymmetric gas-filled cavities.

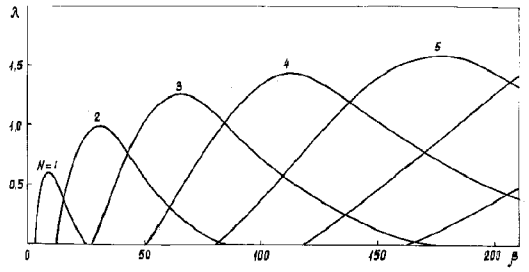

Fig. 26. Real part of the characteristic Eq. (44) roots

When $1 \le \beta < \beta_1^{(1)}$, the steady cavity is asymptotically stable, and when $\beta > \beta_1^{(1)}$, it is unstable. When the parameter β increases and passes through the values $\beta_n^{(1)}$, the oscillations with frequencies $k_n^{(1)}$ are excited. We may suppose that if several frequencies simultaneously exist for the given value of β, the frequency corresponding to the highest coefficient of growth λ becomes dominate when the nonlinear self-induced oscillation of the cavity is establishing. This allows to estimate the limits of modes of the cavity oscillation. A graph of dependence $k(\beta)$ is presented for the first five modes in Fig. 27 (solid lines).

When $\gamma \neq 0$ as in the case of axisymmetric cavities, number of the fundamental cavity frequencies becomes finite. When $\gamma > 0.2153$, the cavity is asymptotically stable for any values of β. According to the data [6] for the stationary cavities past a flat plate perpendicular to the mainstream $\gamma = 2.5 \cdot 10^{-4}$ and effect of taking into account the gas-leakage variability is small.

Table 1. Comparison with experiment (the 1st M.Tulin's scheme)

	Unbounded flow				Jet H = 0.254 m				Experiment [6]	
	$\beta_N^{(1)}$	$\beta_N^{(2)}$	$k_N^{(1)}$	$k_N^{(2)}$	l_j / H	l_j / l_0	$\beta_N^{(1)}$	$\beta_N^{(2)}$	β_N	k_N
	3.081	15.40	4.810	7.088	1.875	0.589	2.226	9.485	5.06	6.15
	15.40	42.70	11.28	13.38	2.125	0.515	8.418	22.48	16.1	12.9
	42.70	83.60	17.74	19.64	2.000	0.551	23.97	46.51	33.5	18.8
	83.60	138.1	24.12	25.90	2.000	0.551	46.51	76.55	55.5	22.9
	138.1	206.5	30.47	32.17	1.875	0.589	81.74	122.0	88.7	30.3

The experiments [6] were carried out in a falling jet with the width H = 25.4 cm at the decreased external pressure p_∞. Closeness of the free boundaries of the flow results in decreasing both the length l_j and the volume Q_j of the steady cavity. According to the relations (45) this should affect on the parameter β values. Using the results of the work [28], we obtain the estimation of influence of the jet boundaries on the "pure" supercavity volume when $\sigma \to 0$:

$$\frac{Q_j}{Q_0} \approx \frac{l_j}{l_0}, \qquad \frac{l_j}{l_0} = \frac{l_j}{H} \Big/ \sinh \frac{l_j}{H}.$$

Table 1 represents theoretical values of the parameters β and k for unbounded flow which correspond to the limits of the cavity pulsation modes The parameter β values are recalculated by formulae (45) with taking account of influence of the jet boundaries.

A graph of the theoretical dependence $k(\beta)$ with taking account of the jet boundaries for five modes of the cavity pulsation are plotted in Fig. 27 by dotted lines. Experimental points from [6] also are plotted there by circles. We have a good agreement with taking account of the experimental data dispersion.

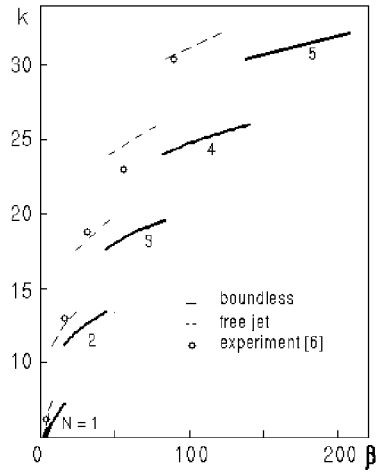

Fig. 27. Modes of the two-dimensional supercavity pulsation

In our work [21], we have investigated stability of the 2-D ventilated supercavities in a free jet with using the 2nd linearized M.Tulin's scheme with the infinite wake and limited pressure at the infinity. We shown that the dynamic properties of both the cavitation schemes are identical.

6.3 THE 2-D SUPERCAVITY SHAPE AT SINUSOIDAL TIME PERTURBATIONS

Now we describe a method of calculation of the length and the shape of the unsteady 2-D supercavity with using the integral Eqs. (36) and (39).

The set of the equations (36), (39) and (4) is nonlinear one, if the cavity length $l(t)$ is considered as an unknown time function. The cause is that variation of the function $l(t)$ has order $l(t) \sim O(1)$ even if $\sigma \sim O(\varepsilon)$ and $\varphi_y(x,t) \sim O(\varepsilon)$, where ε is the small parameter.

We consider a practically important case of periodical dependence of the flow on time [22]. Let the upper wedge side oscillates and deforms sinusoidally

$$f(x,t) = \alpha x + \kappa \operatorname{Re}\{f^*(x)e^{jkt}\}, \tag{46}$$

where $\alpha \sim \kappa \sim O(\varepsilon)$. Here and below, values which are complex with respect to j, are marked by the star. These are named the complex amplitudes.

In the Eq. (36), we replace the time derivative inside the integral and use exponential representation for the time functions with variation of order $O(\varepsilon)$:

$$\begin{gathered} q(x,t) = \alpha q_0(x,l) + \kappa \operatorname{Re}\{q^*(x)e^{jkt}\},\ \sigma(t) = \alpha\sigma_0(l) + \kappa \operatorname{Re}\{\sigma^* e^{jkt}\}, \\ F(x,t) = \alpha F_0(x,l) + \kappa \operatorname{Re}\{F^*(x)e^{jkt}\}. \end{gathered} \tag{47}$$

The first terms in the relations (47) represent quasi-stationary components of the solution, which depend on time only via $l(t)$. The second terms represent non-stationary perturbed components of the solution.

One can show that replacing the time derivative inside the integral and also representation of the solution in the form (47) is equivalent to neglecting some terms. The effect of the latter is essentially decreased with increasing the average cavity length l.

Substituting the expressions (47) into the Eqs. (36) and (39), we obtain a set of the singular integral equations with respect to the complex amplitudes $q^*(x) = q_1(x) + jq_2(x)$ and $\sigma^* = \sigma_1 + j\sigma_2$:

$$\int_1^{l(t)} q^*(s)\left(\frac{1}{x-s} + jk\ln|x-s|\right)ds - \pi\sigma^* = A_1^*(x), \tag{48}$$

$$\int_1^{l(t)} q^*(s)ds = A_2^*, \tag{49}$$

where $A_1^*(x)$, $A_2^*(x)$ are known. When k = 0, we obtain from the Eqs. (48) and (49) the equations to determine the quasi-stationary components $q_0(x)$, σ_0.

We consider the cavity length $l(t)$ as a free time parameter and determine it at the sequential times $t^{(n)} = t^{(n-1)} + \Delta t$ by numerical solving the equation of the mass of gas in the cavity balance (4). In this case the unsteady cavity volume $Q(t^{(n)})$ is calculated by integrating the expression (38). Using the Eq. (38) for the sinusoidal oscillation, we have

$$F^*(x) = \frac{1}{2}e^{-jkx}\int_0^x q^*(s)e^{jks}ds. \tag{50}$$

For each iteration, both the quasi-stationary and the non-stationary parts of the solution are calculated at the same fixed value $l^{(n)}$ from the set of Eqs. (48) and (49) by the numerical method of discrete singularities [24].

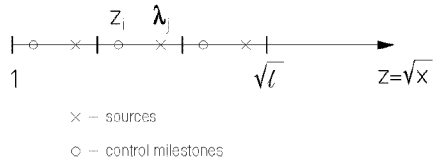

Fig. 28. Discretization of the problem

The numerical method of discrete singularities consists in approximation of the integral Eqs. (48) and (49) by a set of linear algebraic equations. In this case the continuous distribution of sources along the x-axis is replaced by discrete one, and then the quadrature formula of rectangles is applied. Change of variables $x \to z^2$, $s \to \lambda^2$ is preliminarily realized in the integrals to improve the method convergence [24]. The cavity projection is divided into M equal intervals. A point source and a collocation point (control milestones) are located in each interval. The boundary condition (24) is satisfied at the collocation points. Order of location of singularities λ_j and collocation points z_i is determined by the

class of the solution of the singular integral Eq. (48). This solution must be limited at the point of the cavity separation $x = 1$, and it is unlimited at the point $x = l^{(n)}$:

$$z_i = 1 + \Delta z(i - 0.75), \quad \lambda_j = 1 + \Delta z(j - 0.25)\ \Delta z = \frac{\sqrt{l^{(n)}} - 1}{M}, \qquad i, j = 1, 2, \ldots, M. \tag{51}$$

A scheme of the problem discretization is shown in Fig. 28 when $M = 3$.

As a result, separating the real part and the imaginary part, we obtain a set of $2(M + 1)$ linear algebraic equations:

$$\Delta z \sum_{j=1}^{M} \left(\frac{q_{1j}^{(n)}}{z_i^2 - \lambda_j^2} - k q_{2j}^{(n)} \ln \left| z_i^2 - t_j^2 \right| \right) t_j - \frac{\pi}{2} \sigma_1^{(n)} = \frac{1}{2} A_{1,1}^{(n)}(z_i), \qquad i = 1, 2, \ldots, M,$$

$$\Delta z \sum_{j=1}^{M} \left(\frac{q_{2j}^{(n)}}{z_i^2 - \lambda_j^2} - k q_{1j}^{(n)} \ln \left| z_i^2 - t_j^2 \right| \right) t_j - \frac{\pi}{2} \sigma_2^{(n)} = \frac{1}{2} A_{1,2}^{(n)}(z_i), \qquad i = 1, 2, \ldots, M,$$

$$\Delta z \sum_{j=1}^{M} q_{1j}^{(n)} \lambda_j = \frac{1}{2} A_{2,1}^{(n)}$$

$$\Delta z \sum_{j=1}^{M} q_{2j}^{(n)} \lambda_j = \frac{1}{2} A_{2,2}^{(n)}$$

Fig. 29 shows the characteristic wave-like shape of the cavity past the wedge when its sides are performing pitching oscillations about the nose

$$f^*(x) = x$$

for three values of the reduced frequency k.

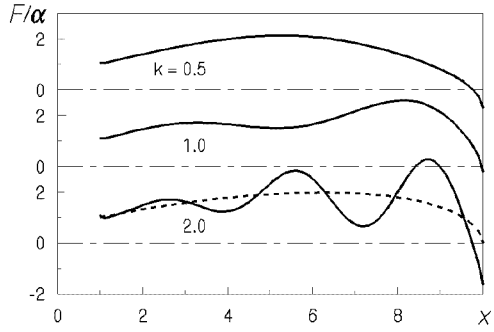

Fig. 29. The cavity shape in dependence on the oscillation frequency: $l_0 = 10.0$, $\overline{\kappa} = 0.1$

In each case the cavity shape was calculated by the Eqs. (47) and (50) at the time t_k when $l(t_k) = l_0$ for convenience of comparison. A shape of the closed stationary supercavity when $k = 0$ is shown by dashed line. When $k > 0$, the cavity is unclosed.

Character of the cavity deformation is the same for different types of oscillations of the wedge. Kinematic waves, which are formed by oscillation of the points of the cavity boundary separation, move along the cavity with the velocity V_∞. Their amplitude increases approximately by linear law.

Graphs of the functions $l(t)$ and $Q(t)$, which are calculated for only period of the oscillation and various values of the relative amplitude $\bar{\kappa} = \kappa / \alpha$, are given in Fig. 30. The wedge sides are wave-likely deformed according to the law (for the upper side):

$$f^*(x) = xe^{-jkx}.$$

One can see that the cavity length oscillation distinguishes more and more from sinusoidal one when the amplitude $\bar{\kappa}$ increases. The same occurs when the reduced frequency k increases. The functions $l(t)$ and $Q(t)$ become discontinuous when $\bar{\kappa}$ and/or k exceed the some critical values.

Fig. 31 shows time dependence of the axisymmetric cavity length and volume that calculated with the code PULSE. Here, a cause of the cavity unsteady perturbation is the ambient pressure oscillation:

$$\beta(t) = \beta_0(1 + \bar{\kappa}\cos kt).$$

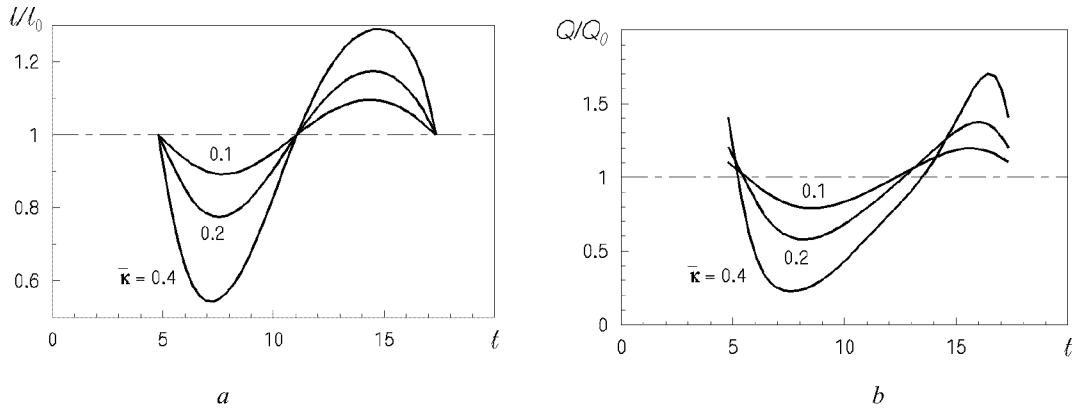

Fig. 30. Influence of the oscillation amplitude on the functions $l(t)$ (a) and $Q(t)$ (b): $l_0 = 6.0$, $k = 0.5$ (wave-like deformation of the wedge)

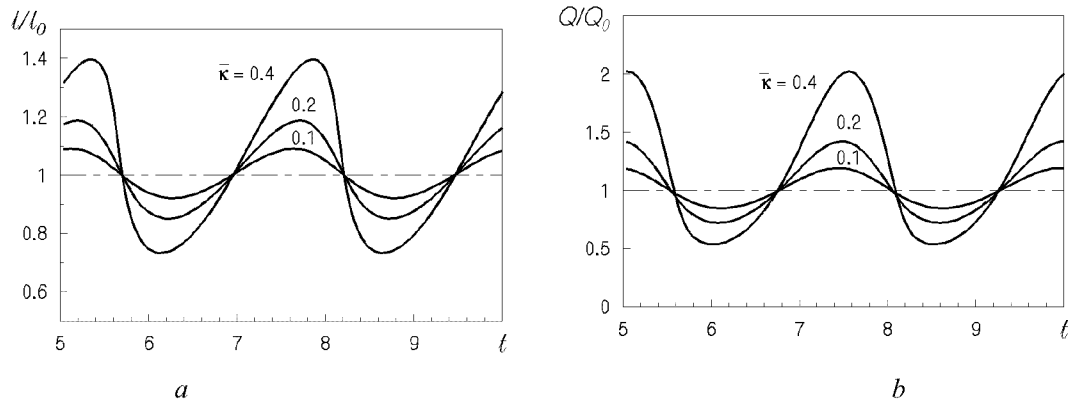

Fig. 31. History of the length (a) and the volume (b) of the axisymmetrical supercavity: $\beta_0 = 1.0$; $k = 2.5$ (the ambient pressure pulsation)

A comparison of graphs in Figs. 30 and 31 shows that shape of the graphs of $l(t)$ and $Q(t)$ for the axisymmetric and the two-dimensional cavities is qualitatively similar in the case of nonlinear

oscillations. When the oscillation frequency and amplitude increases, their shape more and more deviates from sinusoidal one having a shape of a "falling wave". When the frequency and/or the amplitude exceed some critical values k_{cr} and $\overline{\kappa}_{cr}$, the functions $l(t)$ and $Q(t)$ become discontinuous.

The same kind of behaviour of the unsteady supercavities is observed at the experiments for both the axisymmetric and two-dimensional cavities [29].

References

1. Savchenko, Yu.N., Vlasenko, Yu.D. and Semenenko, V.N., Experimental Study of High-Speed Cavitated Flows, *Int. J. of Fluid Mechanics Research*, 1999, **26**, No. 3, pp. 365-374.

2. Savchenko, Yu.N., Semenenko, V.N., and Putilin, S.I., Unsteady Supercavitated Motion of Bodies, *Int. J. of Fluid Mechanics Research,* 2000, **27**, No. 1, pp.109-137.

3. Logvinovich G.V., *Hydromechanics of Free-Boundary Flows*, Halsted Press, 1973.

4. Epshtein, L.A., *Methods of Theory of Dimensionality and Similarity in Problems of Ship Hydromechanics*, Sudostroenie Publishing. House, Leningrad, 1970 [in Russian].

5. Korolyev, V.I., Vlasenko, Yu.D., and Boyko, V.T., Experimental Investigation of the Cavity Development at Unsteady Gas Cavitation, *Gidromehanika*, 1973, No. 24, pp. 79-83 [in Russian].

6. Silberman, E., Song, C.S. Instability of Ventilated Cavities , *J. of Ship Res*., 1961, **5**, No. 1, pp. 13-33.

7. Michel, J.M., Ventilated Cavities. A Contribution to the Study of Pulsation Mechanism, *Unsteady water flows with high velocities, Proc. of International Symp. IUTAM*, Nauka Publishing House, 1973, pp. 343-360.

8. Paryshev, E.V., Theoretical Investigation of Stability and Pulsations of Axially Symmetric Cavities, *Trudy TsAGI,* 1978, No. 1907, pp. 17-40 [in Russian].

9. Paryshev, E.V., Numerical Modeling of Ventilated Cavity Pulsations, *Trudy TsAGI,* 1985, No. 2272, pp. 19-28 [in Russian].

10. Knapp, R.T., Daily, J.W., Hammitt, F.G., *Cavitation*, McGraw-Hill, New York, 1970.

11. Zhuravlyev, Yu.F., Methods of Theory of Perurbations in Three-Dimensional Jet Flows, *Trudy TsAGI,* 1973, No. 1532, pp. 8-12 [in Russian].

12. Savchenko, Yu.N., Semenenko, B.H. Wave Formation on the Boundaries of Cavities Forming at Water Entry of a Disk and Cones, In: *Problems of High-speed Fluid Mechanics,* Chyvashi University Press, Cheboksary, 1993, pp. 231-239 [in Russian].

13. Logvinovich, G.V., Syeryebryakov, V.V., On Methods of Calculations of Slender Asisymmetric Cavities, *Gidromehanika,* 1975, No. 32, pp. 47-54 [in Russian].

14. Semenenko, V.N., Computer Simulation of Dynamics of Supercavitating Bodies, *Prykladna gidromehanika,* 2000, **2**, No. 1, pp. 64-69 [in Russian].

15. Semenenko, V.N., Computer Modeling of Pulsations of Ventilated Supercavities, *Int. J. of Fluid Mechanics Research*, 1996, **23**, Nos. 3 & 4, pp. 302-312.

16. Semenenko, V.N., Computer Simulation of the Unsteady Supercavitating Flows, *High Speed Body Motion in Water (AGARD Report 827), Proc. Fluid Dynamics Panel Workshop*, Kiev, 1997.

17. Elsgolts, L.E., Norkin, S.B., *Introduction in Theory of Differential-Delay Equations*, Nauka Publishing House, Moscow, 1971 [in Russian].

18. Logvinovich, G.V., Yakimov Yu.L., High-Speed Immersion of Bodies in Fluid, *Unsteady water flows with high velocities, Proc. of International Symp. IUTAM*, Nauka Publishing House, Moscow, 1973, pp. 85-92.

19. Semenenko, V.N., Instability of a Plane Ventilated Supercavity in an Infinite Stream, *Int. J. of Fluid Mechanics Research*, 1996, **23,** Nos. 1 & 2, pp. 134-143.

20. Semenenko, V.N., Instability and Oscillation of Gas-Filled Supercavities, *Proc. Third International Symp. on Cavitation,* Grenoble (France), 1998, **2,** pp. 25-30.

21. Semenenko, V.N., Instability of a Plane Ventilated Supercavity in an Free Jet, *Prykladna gidromehanika,* 1999, **1**, No. 2, pp. 45-52 [in Russian].

22. Semenenko, V.N., Calculation of Shape of Plane Supercavities at Harmonic Oscillations, *Prykladna gidromehanika,* 2000, **2**, No. 3, pp. 87-93 [in Russian].

23. Tulin, M.P., Supercavitating Flows – Small Perturbation Theory, *J. of Ship Research,* 1964, **7,** No. 3, pp. 16-37.

24. Yefremov, I.I. *Linearized Theory of Cavitation Flow,* Naukova Dumka Publishing House, Kiev, 1974 [in Ukrainian].

25. Gakhov, F.D., *Boundary value problems,* 3rd Revised and Supplemented Edition, Fizmatgiz Publishing House, 1977 [in Russian].

26. Semenenko, V.N., Unsteady Flow Calculations Past Ventilated Hydrofoils, *Proc. Seventh International Conf. on Numerical Ship Hydrodynamics,* Nantes (France), 1999.

27. Abramovitz, M., Stegun, I. (Editors), *Handbook of mathematical functions with formulae, graphs and mathematical tables*, National Bureau of Standards, Applied Mathematics Series, 1964.

28. Epshtein, L.A., Lapin, V.M. Approximate calculation of influence of Flow Boundaries in Two-Dimensional Problem and past an Axisymmetric Body, *Trudy TsAGI,* 1980, No. 2060, pp. 3-24 [in Russian].

29. Nishiyama, T., Unsteady Cavity Flow Model for Two Dimensional Super-cavitating Hydrofoils in Oscillation, *Technology Reports*, Tohoku Univ., 1982, **46,** No. 2, pp. 199-216.